JOURNAL OF MATERIALS SCIENCE 25 (1990) 1824–1832

HIP-sintered β- and mixed α–β sialons densified with Y_2O_3 and La_2O_3 additions

PER-OLOF OLSSON, THOMMY EKSTRÖM
Department of Inorganic Chemistry, Arrhenius Laboratory, University of Stockholm, S-106 91 Stockholm, Sweden

Various fully dense sialon materials sintered by the glass-encapsulated hot isostatic pressing technique were synthesized using Y_2O_3 and/or La_2O_3 as sintering aids. Constant molar amounts of the oxide mixtures were added in the ratios Y_2O_3/La_2O_3 : 100/0, 75/25, 50/50, 25/75, 0/100. The samples were sintered at two different temperatures, 1550 and 1825° C. At the lower temperature, unreacted α-Si_3N_4 was present in the samples in addition to β-sialon and secondary phases. The samples sintered at 1825° C showed that yttrium but not lanthanum favoured α-sialon formation. The amount of intergranular phase increased by about 50% when Y_2O_3 was replaced by La_2O_3. The La-sialon ceramics have as good an indentation fracture toughness as the Y-sialon ceramics, about 5 MPa $m^{-1/2}$, but the Vicker's hardness is slightly lower, being 1400 kg mm^{-2} at a 98 N load.

1. Introduction

Silicon nitride materials have attracted much interest during the last 30 years due to their good high-temperature mechanical properties [1]. These properties depend on the density of the material, and various oxides must be present as sintering aids for the density to approach the theoretical value. Pressureless sintering of sialon ceramics with additions of Al_2O_3/AlN and a glass-forming metal oxide such as Y_2O_3 has been a successful route. Because Y_2O_3 is rather expensive, however, many oxides have been proposed as replacements for Y_2O_3 as a sintering aid, e.g. CeO_2 [2], Nd_2O_3 [2, 3], MgO [4], ZrO_2 [5] and La_2O_3 [2].

Phase relations in various parts of the five-component La–Si–Al–O–N system have been reported by several authors [6–8]. The results of these investigations are tentatively summarized in the Jenecke-prism shown in Fig. 1. By comparing the La–sialon system with the corresponding Y– [9] and Nd–sialon systems [2, 3] it can be seen that most of the phases found in those two latter systems, including quaternary phases such as N–YAM ($M_4O_6 \cdot Si_2N_2O$, M a metal ion), *N*-α-wollastonite ($M_2O_3 \cdot Si_2N_2O$) and *N*-apatite ($M_{10}(SiO_4)_6N_2$) are also present in the lanthanum system. However, there are some points still in question, such as, whether or not melilite ($M_2O_3 \cdot Si_3N_4$) exists in the La–sialon system. Mitomo *et al.* [7] could not find this phase, contrary to the earlier results by Marchand *et al.* [10]. There also appears to be an unusually large glass-forming region that even reaches the Si_3N_4–La_2O_3 line [7].

The two most important sialon phases, α and β, have structures based on α- and β-Si_3N_4 with aluminium and oxygen partially replacing silicon and nitrogen [11, 12]. The general formula of the α-phase is $M_x(Si, Al)_{12}(O, N)_{16}$, where M has been reported to be lithium, magnesium, calcium, yttrium, and the lantanoids excluding lanthanum, cerium, praseodymium and europium. The stabilizing cation is coordinated to seven (O, N)-positions. In the La-sialon system, no α-phase has been reported, probably due to the large radius of the La^{3+} ion. The effective ionic radius (based on the radius of oxygen in the rock-salt structure being equal to 0.140 nm) of the seven-coordinated La^{3+} ion is, according to Shannon and Prewitt [13], equal to 0.110 nm. The largest ion able to stabilize the α-sialon structure seems to be Nd^{3+} [2]. No value is given for the seven-coordinated Nd^{3+} ion by Shannon and Prewitt, but it is possible to estimate the radius to be about 0.104 nm by comparing the sizes of the six- and eight-coordinated lanthanum and neodymium ions. The β-phase, on the other hand, does not incorporate other cations. The composition of this phase is given by the formula $Si_{6-z}Al_zO_zN_{8-z}$, with z varying from 0 (Si_3N_4) to a maximum value of about 4.2 depending on sintering conditions [14].

There have been only a few investigations of the use of La_2O_3 as a sintering aid for Si_3N_4 [15–18] and even less for sialons [17]. From the Si_3N_4 studies some interesting results have emerged, such as relatively good high-temperature hardness [15] and lower liquid-formation temperature during sintering than for yttrium-doped materials [16]. These observations and the fact that a relatively high density has been achieved for the Si_3N_4 material sintered with La_2O_3 [17, 18] show that lanthanum oxide could be a good alternative to Y_2O_3 as a sintering aid for sialon materials.

The present investigation forms a part of a larger research project where possible replacement of Y_2O_3 by other oxides in sialon ceramics is being studied. This also includes studies of Nd_2O_3 [3] and CeO_2 [19]. In this article the properties of fully dense lanthanum-doped sialons synthesized by the glass-encapsulated hot isostatic pressing (HIP) technique are reported and discussed.

0022–2461/90 $03.00 + .12

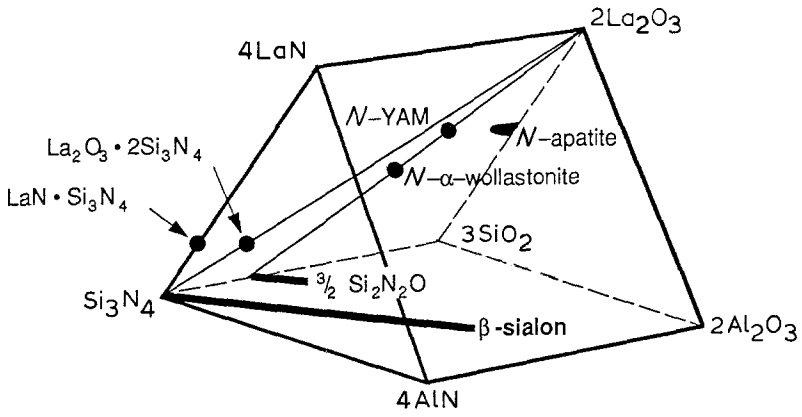

Figure 1 A schematic representation of the La–Si–Al–O–N system.

2. Experimental details

The selected compositions investigated in this study are shown in Fig. 2. Equivalents are defined by the following formulae

$$\text{equiv. Al} = \frac{3 \times (\text{at \% Al})}{3 \times (\text{at \% Al}) + 4 \times (\text{at \% Si})}$$

and

$$\text{equiv. O} = \frac{2 \times (\text{at \% O})}{2 \times (\text{at \% O}) + 3 \times (\text{at \% N})}$$

Oxygen from the added Y_2O_3 or La_2O_3 is not included in the calculations of the oxygen equivalents. The chosen compositions are situated close to the Si_3N_4 corner of the M–Si–Al–O–N phase diagram, comprising two samples that contain only β-sialon and liquid (nos 1, 4) and three samples (nos 2, 3, 5) which fall in the α–β part of the Y-sialon system.

A constant molar fraction of (Y_2O_3 + La_2O_3) was added to all samples, corresponding to 6.0 and 8.7 wt % for the pure Y_2O_3 and La_2O_3 specimen, respectively. The samples were prepared with mixtures of Y_2O_3/La_2O_3 in the ratios 100/0, 75/25, 50/50, 25/75 and 0/100. The source materials used were silicon nitride (H. C. Starck-Berlin, LCI), aluminium oxide (Alcoa, A16SG), aluminium nitride (H. C. Starck-Berlin, Grade A), yttrium oxide (H. C. Starck-Berlin, 99.9%) and lanthanum oxide (Johnson Matthey Chem. Ltd, 99.9%). The analysed oxygen content of the silicon nitride corresponds to 2.9 wt % SiO_2 and the oxygen content of the aluminium nitride to 1.9 wt % Al_2O_3.

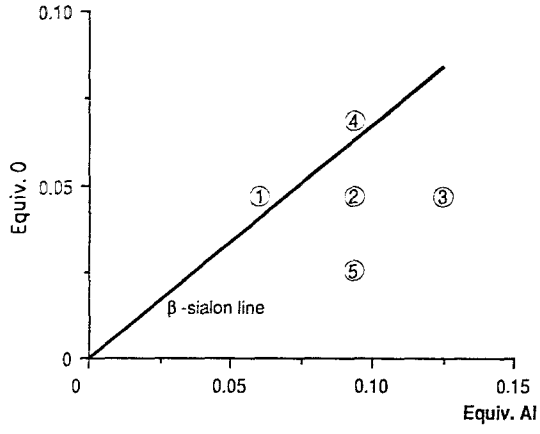

Figure 2 The overall compositions of the samples made in this study represented as equivalents of oxygen and aluminium added to Si_3N_4.

The starting powders were carefully weighed, taking account of the extra oxygen present on the surface of the nitride particles. The materials were synthesized on the semi-pilot plant scale, i.e. the batch size was 500 g dry weight. The starting materials were mixed in water-free propanol and milled in a vibratory mill for 16 h with sialon milling medium. After drying, the powder mixes were dry pressed (125 MPa) into compacts of size 16 × 16 × 6 mm. The specimens were protected by a thin coating of BN powder and hot-isostatically pressed under 200 MPa pressure of argon gas [20] at 1550 or 1825° C for 2 h, using a glass-encapsulation technique. The reference letter L following the sample number refers to firing at 1550° C and the letter H to 1825° C.

Density measurements using Archimedes' principle were made with a precision of $\pm 0.002\,\text{g cm}^{-3}$. The limits of accuracy obtained from different specimens of the same composition is about ±0.01, however. The sintered material was prepared for physical characterization by grinding and polishing using standard techniques. Special care was taken in the final polishing step to minimize any material pull-out and to minimize any influence of introduced compressive stresses on subsequent physical measurements. Hardness (HV10) and indentation fracture toughness (K_{Ic}) at room temperature were obtained by a Vickers' diamond indentor using a 98 N (10 kg) load, and the fracture toughness was evaluated with the method of Anstis *et al.* [21] assuming a value of 300 GPa for Young's modulus. The precision of repeated measurements on the same sample was ±30 and ±0.2 for the HV10 and K_{Ic} values, respectively.

The phase analysis was based on X-ray powder patterns recorded in a Guinier–Hägg focusing camera ($CuK\alpha_1$ radiation, silicon as internal standard with $a = 0.543\,088$ nm [22]. The equations $a = 0.7603 + z' 0.00297$ nm and $c = 0.2907 + z' 0.00255$ nm were used to calculate the z-values for the β-sialon phase [14]. For determining the ratio of α- to (α + β)-sialon present, a simple method, based on the integrated intensities of the (1 0 2) and (2 1 0) reflections of the α-phase and the (1 0 1) and (2 1 0) lines of the β-phase, was used. This and more exact methods have been discussed recently by Käll [23]. Scanning electron microscopy was performed on carbon-coated as-sintered materials, using a Jeol JSM 820 instrument

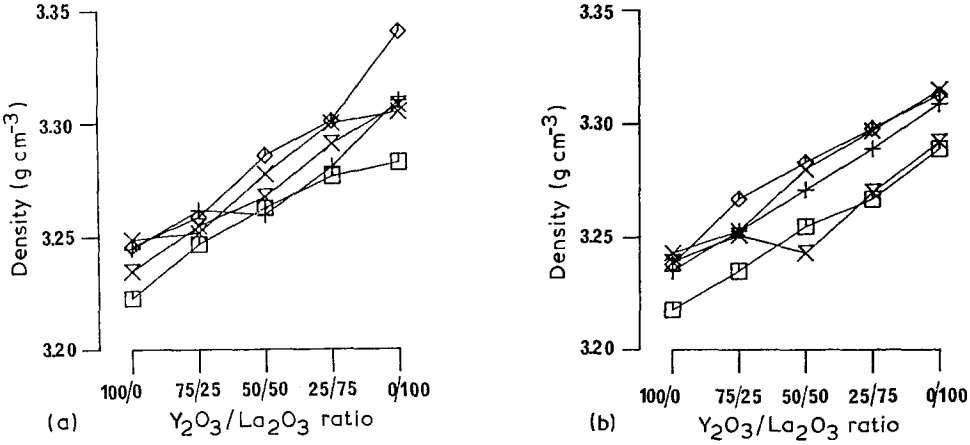

Figure 3 Density variations for the samples HIP-sintered at (a) 1550° C and (b) 1825° C. Samples (x̄) 1, (+) 2, (×) 3, (□) 4, (◇) 5.

equipped with a Link AN 10 000 EDS analyser. The amount of glassy phase was estimated by a simple counting technique using a grid superposed on the micrographs. For the TEM studies a thin plate (< 0.2 mm) was cut with a wire saw and dimpled to a thickness of about 40 μm. The final thinning was made by argon milling. To prevent charging in the microscope, the specimen was covered with an amorphous carbon layer. The TEM investigations were made at 200 kV in a Jeol 200CX microscope equipped with a top-entry, double tilt goniometer.

3. Results

3.1. Density measurements

Examination of the polished cross-sections of the HIP-sintered ceramics by optical microscopy or SEM revealed only a few micropores, indicating that the samples had reached practically theoretical density by the HIP process. The density measurements show a general trend of density increase with increasing lanthanum content (Figs 3a, b). The magnitude of this increase, for the same composition, when changing the sintering aid from Y_2O_3 to La_2O_3 is about 0.07 g cm^{-3}. The samples with composition 5L showed, however, an increase in density as high as about 0.1 g cm^{-3} when changing from Y_2O_3 to La_2O_3. This relatively large change in density could be seen to be accompanied by a drastic change in microstructure and phase composition (see below). When comparing the densities for samples sintered at 1825° C with the same mixture of Y_2O_3–La_2O_3, it was possible to detect a small difference in density between the β-sialon and

TABLE I Phases identified in the samples sintered at 1550° C with the use of X-ray diffraction results obtained by the Guinier–Hägg technique

Sample	Y_2O_3/La_2O_3 ratio	Phases by XRD except β-sialon	$\alpha/\alpha + \beta$ ratio	β-sialon, z	α-sialon	
					a (nm)	c (nm)
1L	100/0	α-Si_3N_4	0.82	0.47	*	
	75/25	α-Si_3N_4, AlN	0.80	1.05	*	
	50/50	α-Si_3N_4, AlN	0.86	0.90	*	
	25/75	α-Si_3N_4	0.82	0.72	*	
	0/100	α-Si_3N_4	0.80	0.62	*	
2L	100/0	α-Si_3N_4, 12H	0.82	0.73	*	
	75/25	α-Si_3N_4, 12H	0.82	0.59	*	
	50/50	α-Si_3N_4, 12H	0.46	0.72	*	
	25/75	α-Si_3N_4, 12H	0.85	0.59	*	
	0/100	α-Si_3N_4, 12H	0.87	0.62	*	
3L	100/0	α-Si_3N_4, 12H	0.82	0.82	*	
	75/25	α-Si_3N_4, 12H	0.82	0.62	*	
	50/50	α-Si_3N_4, 12H	0.85	0.59	*	
	25/75	α-Si_3N_4, 12H	0.88	0.63	*	
	0/100	α-Si_3N_4, 12H	0.33	0.65	*	
4L	100/0	α-Si_3N_4	0.55	0.61	*	
	75/25	α-Si_3N_4, 12H	0.55	1.23	*	
	50/50	α-Si_3N_4, 12H	0.55	1.45	*	
	25/75	α-Si_3N_4, 12H AlN	0.69	1.40	*	
	0/100	α-Si_3N_4	0.12	0.59	*	
5L	100/0	α-Si_3N_4, α-sialon AlN	0.66†	0.27	7.809	5.692*
	75/25	α-Si_3N_4, AlN	0.65†	0.27	7.802	5.677*
	50/50	α-Si_3N_4, AlN	0.91	0.17	*	
	25/75	α-Si_3N_4, AlN	0.84	0.22	*	
	0/100	α-Si_3N_4, $LaSiO_2N$	0.78	0.21	*	

*Sample contains undissolved α-Si_3N_4; a = 0.775 3(2), c = 0.562 1(4).
† Ratio of α-Si_3N_4/(α-sialon + β-sialon + α-Si_3N_4).

the mixed α–β-sialon samples with a high amount of La_2O_3 added.

3.2. X-ray diffraction analysis

XRD analysis revealed clear differences between the materials prepared at the two sintering temperatures, as shown in Tables I and II. The samples sintered at 1550° C (nos xL) contained a large amount of unreacted α-Si_3N_4 for all compositions, which was not the case for the materials sintered at the higher temperature (nos xH). The hexagonal cell parameters for the α-Si_3N_4 phase were found to be $a = 0.775\,3(2)$ nm and $c = 0\,562\,1(4)$ nm, which clearly shows that this is not an α-sialon phase [10] (cf. Table II). In addition to α-Si_3N_4, all the low-temperature HIPed material contained β-sialon. For most of these a fairly constant amount of the α-Si_3N_4 had been converted to the β-sialon phase. Some exceptions to this observation were found in the samples sintered with La_2O_3, e.g. 3L, in which 67% of the silicon nitride based materials were β-sialon, whereas for the other, yttria-containing mixtures in this series only about 15% had formed β-sialon. The secondary crystalline phases observed were Si–Al–O–N polytypes, AlN and some La–silicon oxynitrides. The most frequently observed secondary phase besides α-Si_3N_4 was the 12H Si–Al–O–N polytype. For the two most yttria-rich samples in the 5L series some α-sialon was observed, and $LaSiO_2N$ was present in the 5L sample sintered with the highest amount of La_2O_3. In addition to the X-ray lines that were possible to identify, some additional very weak reflections belonging to some uncharacterized phases were observed.

The β-sialon z-values in the low-temperature series showed a large variation between the five compositions. The lowest z-values, about 0.2 were found in the 5L series. In series 2L and 3L the z-values were about 0.6. The highest z-values, 1.3 to 1.4, were found in the 4L-series, but the 4L sample doped with pure La_2O_3 had a value of only 0.6. Finally, the z-values of the 1L series showed a variation between 1.0 and 0.5.

The samples sintered at (1825° C) did not contain any unreacted α-Si_3N_4. The analysis showed that the samples of series 1H and 4H were pure β-sialon materials regardless of the Y_2O_3/La_2O_3 ratio and contained no other crystalline phases. The sample series 2H, 3H and 5H were α–β-sialons in the pure Y_2O_3-system, but the amount of α-sialon phase decreased with increasing La_2O_3 content until, for pure La_2O_3 additions, no α-sialon could be detected by X-ray diffraction (XRD) analysis. In the 3H series, evidence for the 12H polytype could be found, and its amount increased slightly with increasing La_2O_3 content. A slight tendency to decrease of the z-values could be noted for increasing La_2O_3 additions. However, because the observed variation only corresponds to a minor change in cell parameters (< 0.0005 nm) it was not considered as significant.

3.3. Microstructural studies

Typical microstructures for the low-temperature sintered samples are shown in Fig. 4. It is clearly seen that the size of the grains is small and rarely exceeds 2 to 3 μm. The microstructures of specimens with Y_2O_3/La_2O_3 ratios varying between 100/0 and 25/75 are very similar in appearance, whereas that of the specimen doped with pure La_2O_3 (0/100) is very different in character. In the latter specimens both grain size and

TABLE II X-ray diffraction results obtained by Guinier–Hägg technique of the 1825° C samples

Sample	Y_2O_3/La_2O_3 ratio	Phases by XRD except β-sialon	α/α + β ratio	β-sialon, z	α-sialon	
					a (nm)	c (nm)
1H	100/0	–	–	0.49		
	75/25	–	–	0.47		
	50/50	–	–	0.42		
	25/75	–	–	0.38		
	0/100	–	–	0.39		
2H	100/0	α-sialon	0.30	0.60	7.802	5.684
	75/25	α-sialon	0.12	0.65	7.800	5.671
	50/50	α-sialon	0.10	0.61	7.799	5.672
	25/75	–	–	0.61		
	0/100	–	–	0.49		
3H	100/0	α-sialon w b-phase	0.47	0.69	7.810	5.678
	75/25	α-sialon	0.34	0.72	7.800	5.682
	50/50	α-sialon vw 12H	0.32	0.61	7.804	5.667
	25/75	12H	–	0.54		
	0/100	12H	–	0.54		
4H	100/0	–	–	0.69		
	75/25	–	–	0.70		
	50/50	–	–	0.66		
	25/75	–	–	0.61		
	0/100	–	–	0.73		
5H	100/0	α-sialon vw b-phase	0.58	0.69	7.806	5.680
	75/25	α-sialon	0.47	0.50	7.802	5.672
	50/50	α-sialon	0.33	0.36	7.790	5.671
	25/75	α-sialon	0.18	0.43	7.780	5.661
	0/100	–	–	0.44		

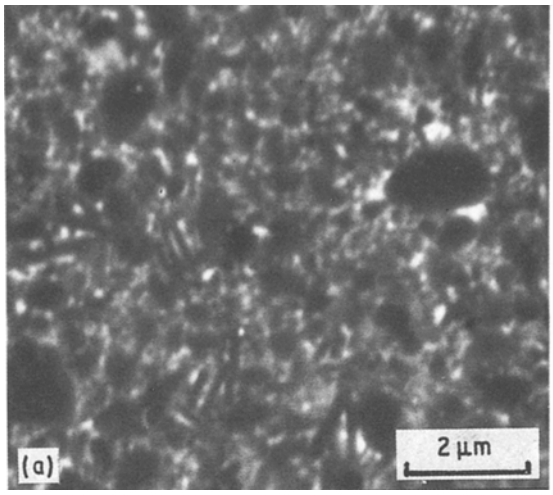

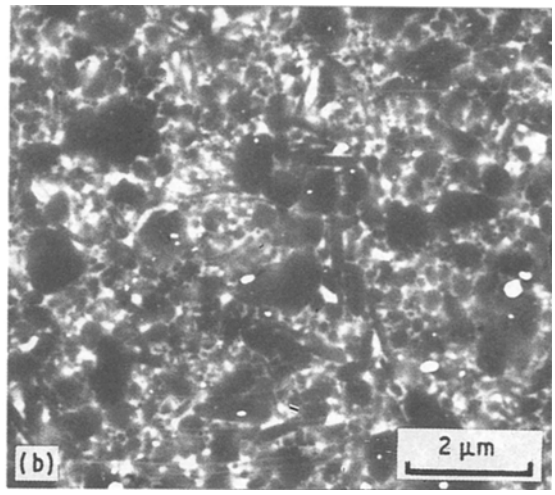

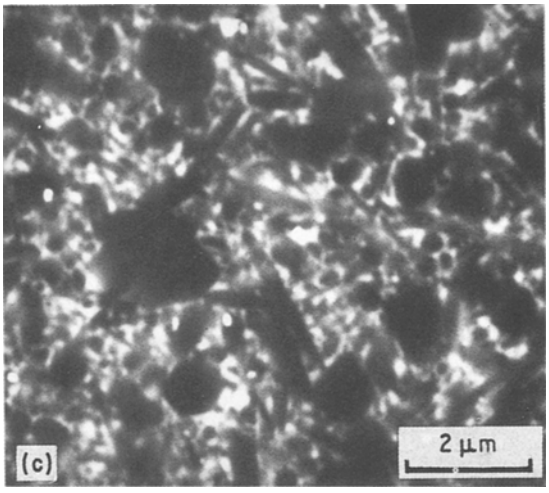

Figure 4 Microstructure of sample series 3L HIP-sintered at 1550° C with the addition of a mixture of Y_2O_3/La_2O_3 in proportions equal to (a) 25/75, (b) 75/25, and (c) 100/0.

amount of intergranular phase are significantly larger, especially for samples 3L and 4L. For example, sample 3L, with only La_2O_3 as sintering aid, contains larger (4 to 5 μm) β-sialon grains (black contrast) than the rest of the 3L samples (2 to 3 μm). The same is true for the 4L samples. For the most lanthanum-rich 5L sample (Fig. 5), light "flowery" areas 30 to 50 μm in diameter could be seen by using backscattered mode. It was also possible to find such areas in a minor amount in the sample containing Y_2O_3/La_2O_3 equal to 25/75. The energy-dispersive X-ray spectrometry (EDS) analysis showed that these areas were rich in lanthanum, compared with the darker areas which contained almost no lanthanum. This result indicates that a segregation had occurred in the material to form lanthanum-rich and lanthanum-deficient areas. The only lanthanum-containing crystalline phase which could be identified with XRD analysis in the most lanthanum-rich sample was $LaSiO_2N$. The amount of intergranular phase in the low-temperature sintered samples showed a tendency to increase with increasing amount of La_2O_3 addition. Thus, an estimate of the amount of intergranular-phase for 3L samples gives about 10 vol % for the 75/25 Y_2O_3/La_2O_3 and about 15 vol % for the pure La_2O_3 samples.

The microstructure of the samples sintered at 1825° C shows a different grain-size distribution compared with the low-temperature series. A typical microstructure of a β-sialon ceramic, represented by sample series 4H, is seen in Fig. 6. It is clear that the β-sialon grains (black) are much larger and more elongated than in low-temperature material. The size of the grains becomes smaller when the La_2O_3 replacement for Y_2O_3 increases. The amount of intergranular phase increases by almost 50% from the 75/25 to the 0/100 sample. An example of an α–β sialon (no. 3H) is seen in Fig. 7. The α-sialon grains, having a grey contrast in the micrograph, are seen to decrease in number with increasing lanthanum content, whereas the amount of β-sialon grains increases. It can be noted that the α-sialon grains have a similar elongated shape as the β-sialon grains.

A TEM image of the microstructure of the 3H sample sintered with pure La_2O_3 at 1825° C is seen at a higher magnification in Fig. 8. The grains are needle-shaped and embedded in an intergranular phase. The grains can be divided into two groups based on the observed size distribution. First a few relatively large grains can be found, with crystal diameters, of about 0.2 to 0.3 μm orthogonal to the growth direction. In addition to these, grains about ten times smaller can

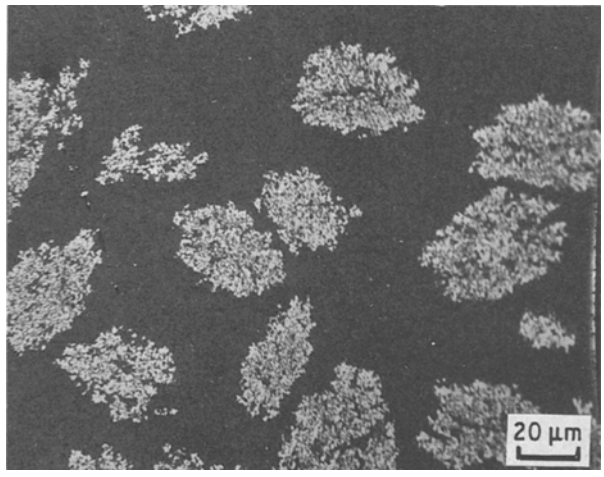

Figure 5 Microstructure of sample 5L sintered at 1550° C with La_2O_3 as sintering aid. The image shows the segregation between lanthanum-rich (light contrast) and lanthanum-poor (dark contrast) areas.

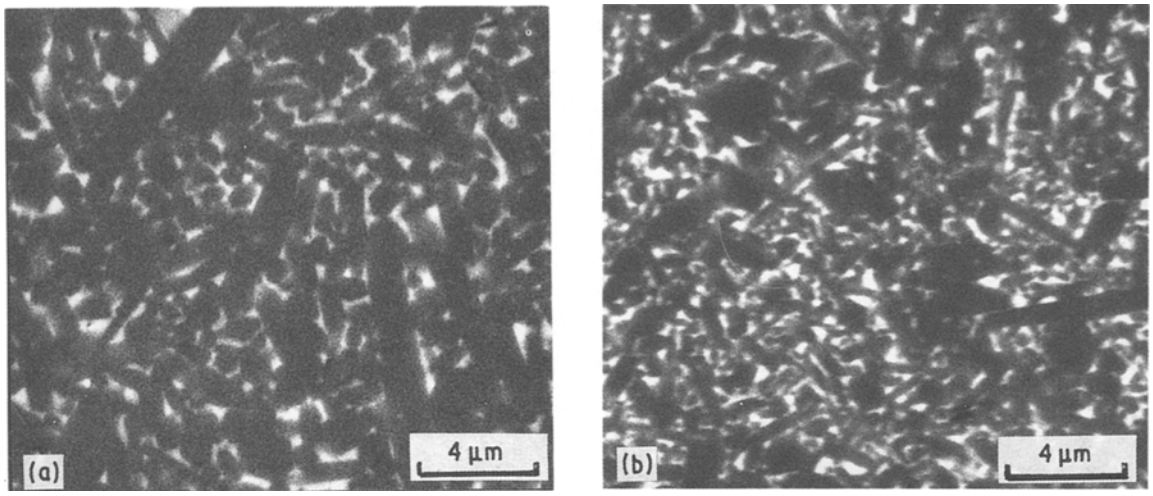

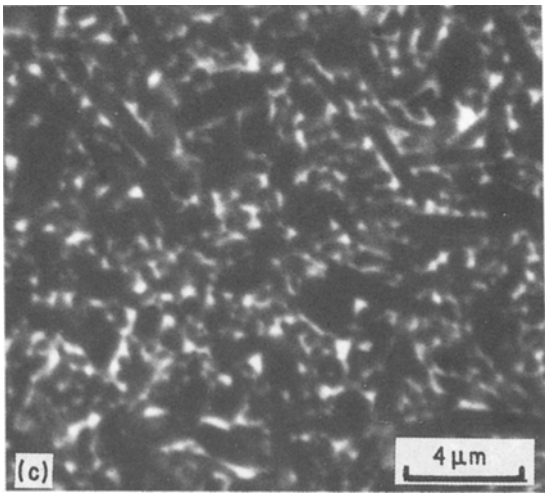

Figure 6 Microstructure of sample series 4H sintered at 1825° C. The samples have been sintered with the addition of a mixture of Y_2O_3/La_2O_3 in proportions (a) 25/75, (b) 75/25, and (c) 100/0. The composition of the series corresponds to a β-sialon in the pure Y–Si–Al–O–N system.

also be observed. One such small grain surrounded by larger grains and embedded in a glassy pocket is seen in Fig. 9. The bright-field (Fig. 9a) and the corresponding dark-field image (Fig. 9b) show that the grains are separated from each other by a thin amorphous film.

The EDS analysis of the β-sialon samples shows that yttrium and lanthanum are always concentrated in the intergranular phase. For the α–β-sialon samples it was possible to detect yttrium in the α-sialon grains, but no lanthanum. Crystals identified by electron diffraction as α-sialon were carefully studied using EDS analysis but gave no lanthanum signal, not even the 5 H sample sintered with a 25/75 mixture of Y_2O_3 and La_2O_3.

3.4. Hardness and fracture toughness

The sintered sialon ceramics could be divided into two principal groups: those which contained only β-sialon and those which contained a mixture of α- and β-sialon phases when sintered with only Y_2O_3 as a sintering aid. The measured Vickers' hardness and indentation fracture toughness of these two principal groups are given in Figs 10 and 11. It is seen that the materials prepared at low temperature (1550° C) and high temperature (1825° C) differ significantly, independent of the composition of the sialon material. The general trend is that low-temperature materials are harder and more brittle (lower fracture toughness).

The changes in hardness or toughness with the Y_2O_3/La_2O_3 ratio are fairly moderate for the β-sialon ceramics 1 and 4 (see Figs 10a and b). At both temperatures a slight drop in hardness can be seen as the amount of La_2O_3 increases; and the most notable change in fracture toughness is from 3.2 to 3.9 for the 1550° C preparation of sample 4. The changes in physical properties of the α–β-sialon ceramics, illustrated in Figs 11a and b, are more distinct, especially for the 1825° C preparations. For these samples a clear drop in hardness with increasing lanthanum content is observed, with a corresponding rise in fracture toughness.

4. Discussion

Examination of the samples in the optical microscope revealed very little porosity, and the variation in the measured densities therefore mainly reflects changes in the amount or density of the phases present. First of all, it is clearly seen that the replacement of Y_2O_3 by La_2O_3 increases the density for all compositions. Other factors might also have some smaller influence on the density. It must, however, be stressed that small changes are difficult to detect because the spread between different specimens of the same composition is about ± 0.01 (see above). One factor that influences the density of the glassy phase is the nitrogen content. It has been reported that a nitrogen-rich glass can be more than 10% heavier than one without nitrogen [24, 25]. Another effect may also be a relative change in the glass volume, and it is expected that the mixed α–β- sialon samples in the pure Y_2O_3 case will have a some what smaller amount of glassy phase than the β-sialons, as the overall compositions are further away from the glass-forming region in the Y–Si–Al–O–N system. The formation of α-sialon consumes a fair amount of sintering aid and as the amount of La_2O_3 is increased no lanthium-stabilized α-sialon is formed. The amount of sintering aid in the glassy phase will therefore increase more rapidly for the α–β-sialons than for the pure β-sialon.

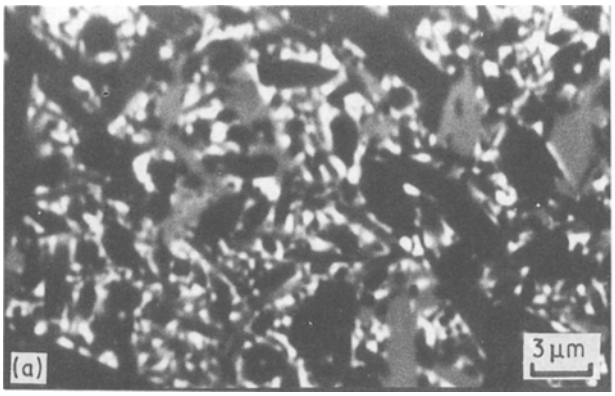

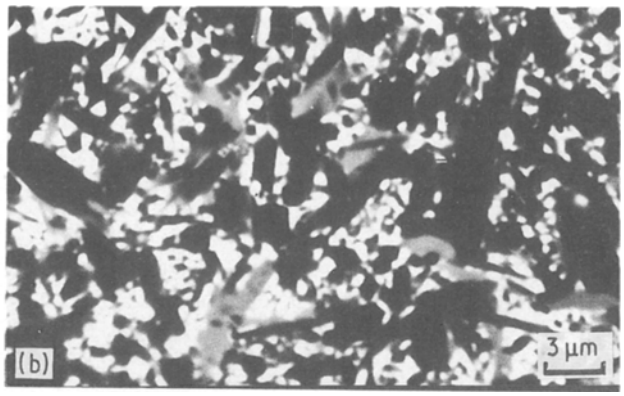

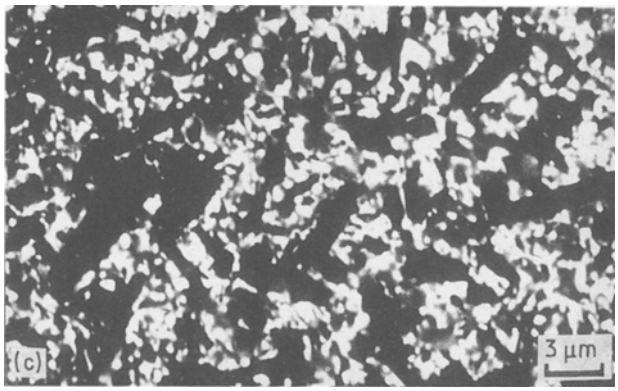

Figure 7 Microstructure of sample series 5H sintered at 1825° C. The samples have been sintered with the addition of a mixture of Y_2O_3/La_2O_3 in proportions (a) 25/75, (b) 75/25, and (c) 100/0. The composition of the series corresponds to a α-β-sialon in the pure Y–Si–Al–O–N system.

Glasses in the La–Si–O–N system have been reported to contain 18 at % nitrogen [26], and as the glass-forming region is expanded when aluminium is added, the La–sialon glass in the present case might contain even more nitrogen. In a recent paper, Korgul and Thompson [27] have shown that glasses of composition $LaSiO_2N$ containing 20 at % nitrogen can be prepared by melting the corresponding α-wollastonite type phase, and it is believed that nitrogen incorporation might be even higher than this.

The increase in overall density observed for both the low- and high-temperature samples with increasing lanthanum content might only partly be explained by the observed increase in the amount of intergranular phase with a density of about 4 [24, 25]. In addition to this, the density of the glass is affected by the higher atomic weight of lanthanum (138.9) compared to yttrium (88.9). The coordination numbers of yttrium and lanthanum are reported to be 8 and 7, respectively [15], which should imply a more expanded glass for yttrium. A typical La–sialon glass of the overall composition (29 eq % La, 16 eq % Al, 56 eq % Si, 17 eq % N, 83 eq % O) has a measured density of 4.55 g cm^{-3}, while the same glass with yttrium replacing lanthanum has a density of 4.1 g cm^{-3} [28]. It can also be mentioned that the former glass has a hardness of only 600 kg mm^{-2} despite the higher density, compared with a value of 1050 kg mm^{-2} for the Y–sialon glass.

The samples sintered at 1550° C for 2 h had obviously not reached equilibrium, because much of the α-Si_3N_4 starting material remained unreacted. The observed variations in the z-value of the β-sialon phase at this temperature have to be interpreted in the light of this fact. The β-sialon phase that crystallizes from the liquid adopts a z-value (degree of Al–O substitution) that depends on the amount of aluminium and oxygen present in the liquid. At 1550° C all of the added Al_2O_3, but only a part of the AlN, will be dissolved and give a contribution to the aluminium concentration in the liquid. The relatively low solubility of AlN at this temperature is evinced by the fact that unreacted AlN was found by XRD analysis in series 1L and 5L. For sample series 4L, Al_2O_3/AlN was equal to 1.32, i.e. most of the added aluminium was in the form of Al_2O_3, whereas for sample series 5L, Al_2O_3/AlN was equal to 0.05. Indeed samples 4L have somewhat higher z-values and sample 5 slightly lower z-values than expected, if the z-values found for the 1825° C materials are used as reference. It might seem surprising in view of this discussion that samples 1 have relatively high z-value despite the presence of AlN in the sintered product. However, in these samples the value of the Al_2O_3/AlN ratio was equal to 0.87 which is the second largest value found in any series. The diffraction results from the 1825° C samples confirm that lanthanum does not stabilize the α-phase. However, it is surprising that the amount of α-sialon phase in our preparations declines so rapidly with increasing La_2O_3 content that even in the "25/75"

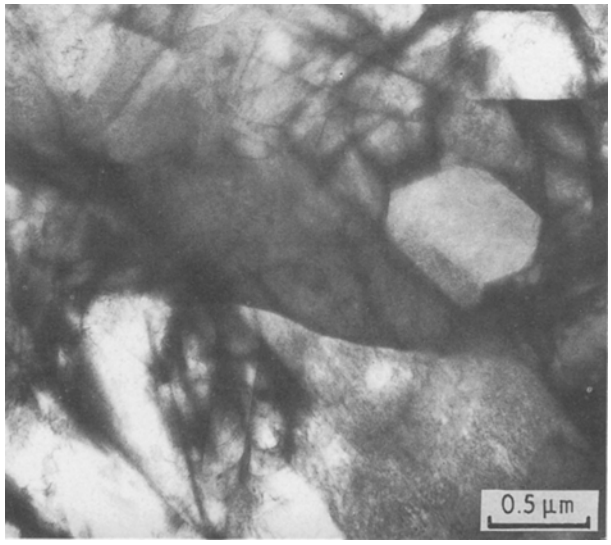

Figure 8 TEM image of the 3H sample sintered with pure La_2O_3 as sintering aid. The micrograph shows the size distribution of β-sialon particles.

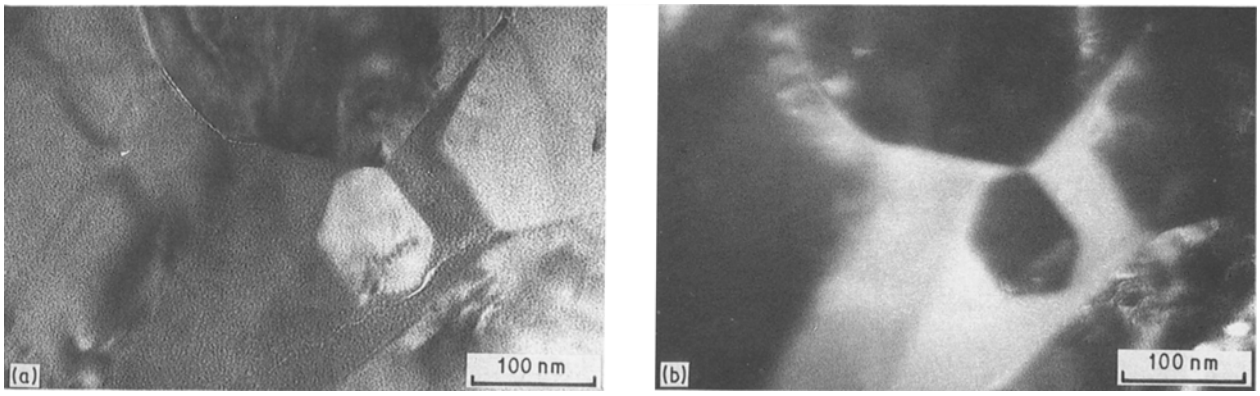

Figure 9 Pocket of fine secondary crystalline grains in the 3H sample sintered with pure La_2O_3 as sintering aid. (a) TEM bright-field image, (b) dark-field using diffusely scattered electrons, showing a thin amorphous film which separates individual grains.

samples of 2H and 3H, where Y_2O_3 is present, no α-sialon is found (see Table II). This could imply that the yttrium-ion has a slight preference for the La–sialon glass over the α-sialon phase, which cannot form without being stabilized by yttria.

The changes in hardness and fracture toughness of the prepared sialon materials might be explained mainly from the obvious shifts in α- to (α + β)-sialon phase ratio and the changes in microstructural features such as grain size, shape and amount of intergranular phase. In the preparations at 1550° C the hardness is high because the grain size is small ($\lesssim 2\,\mu$m), the amount of "soft" glassy phase (HV $\lesssim$ 1000) is less than at 1825° C, and the materials contain a reasonable amount of the hard α-Si_3N_4 phase. The slight drop in hardness with increasing La_2O_3 content is probably due both to the increasing amount of glassy phase and to the fact that lanthanum-containing glass is softer. The low toughness of the low-temperature preparations is mainly due to the fact that crystals of an elongated shape have been unable to form and that a large part of the grains is unreacted starting material of a rather chunky shape. However, it was observed by SEM that the two samples from the series 3L and 4L, containing only La_2O_3 as sintering aid, contained some β-grains that had started to grow slightly larger and in a more elongated shape. This indicates that the liquid phase in the pure La–sialon system for series 3L and 4L favours the transformation of α-Si_3N_4 to β-sialon and hence crystal growth.

The grain size of the high-temperature materials is larger, and so is the amount of intergranular phase, which satisfactorily explains the lower hardness values generally observed. In addition to this, the phase composition is also of importance. Although no unreacted α-Si_3N_4 is present in the samples sintered at 1825° C, the isostructural α-sialon is formed. The hardness is clearly higher in the α–β-sialon materials compared with the β-sialon materials, which is a consequence of the well-known fact that the α-sialon is harder than the β-sialon phase [29]. The clear drop in hardness observed for the α–β sialon ceramics (nos 2, 3, and 5) with increasing La_2O_3 content is therefore mainly due to the reduced amount of α-sialon, in addition to the increased amount of glass. It is interesting to note that at high La_2O_3 contents, when no α-sialon is present, the hardness is about the same as for the β-sialon ceramics 1 and 4. The fracture toughness is generally high for the 1825° C preparations as a consequence of the elongated shape of the β-sialon grains. The α-sialon phase does not typically form elongated crystals in the case of pure Y–sialons, which means that the highest fracture toughness values in the Y–sialons are found in those materials that contain only β-sialon, e.g. sample series 1 and 4. With Y_2O_3–La_2O_3 additions we have, however, noted a tendency also for the α-grains to grow in a more elongated shape, but in these

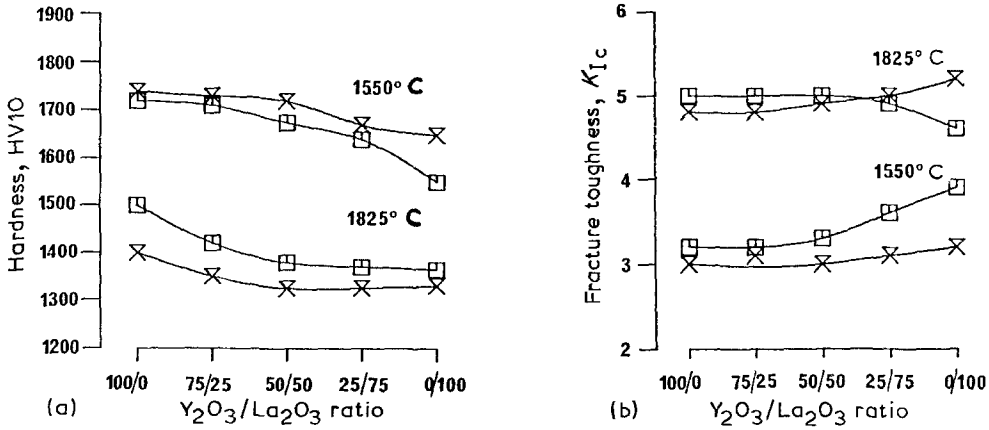

Figure 10 The measured mechanical properties of the β-sialon ceramics. (a) The Vickers' hardness HV10 (kg mm^{-2}) at a 98 N load and (b) the indentation facture toughness, K_{Ic} (MPa m$^{-1/2}$). Samples: (×) 1, (□) 4.

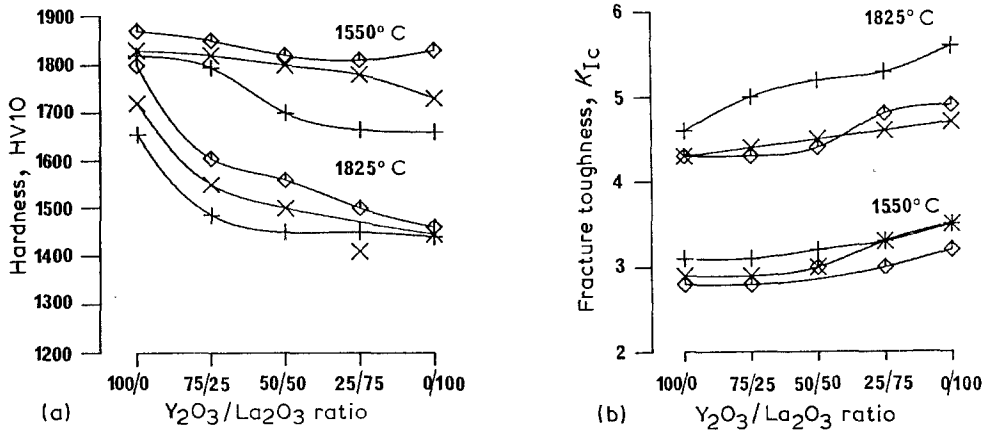

Figure 11 The mechanical properties of the α-β-sialon ceramics as in Fig. 10. Samples: (+) 2, (×) 3, (◇) 5.

samples the $\alpha/(\alpha + \beta)$ ratio simultaneously decreases with increasing La_2O_3 content.

We have not been able to identify any secondary phases by XRD analysis except small amounts of the 12H polytypoid and the b-phase (Y_2SiAlO_5N) in the high-temperature sintered samples. This contrasts with a corresponding investigation of the neodymium system [3], which showed that substantial amounts of melilite were formed. Our results are, however, in agreement with the finding, by Mitomo *et al.* [4] that the melilite phase does not form in the La-sialon system.

In this study an HIP technique has been used to ensure formation of fully dense sialon samples. Measurements of fracture toughness show that La-sialons can be obtained with properties as good as those of the corresponding Y-sialon ceramics. This has encouraged us to initiate further studies which include preparation of these materials using a pressureless sintering route, which is less expensive than the HIP technique. The results of that project will be published in a forthcoming communication.

Acknowledgements

We are grateful for permission from AB Sandvik Hard Materials to publish this article. This work has in part been financed by the Swedish Board for Technical Development and in part by AB Sandvik Hard Materials. Dr M. Pomeroy of Limerick and Dr D. P. Thompson are thanked for their interest and stimulating comments on the manuscript.

References

1. K. H. JACK, *Metals Technol.* **9** (1982) 297.
2. S. SLASOR, K. LIDDELL and D. P. THOMPSON, *Br. Ceram. Proc.* **37** (1986) 51.
3. T. EKSTRÖM, P.-O. KÄLL, M. NYGREN and P.-O. OLSSON, *Mater. Sci. Engng* **A105/106** (1988) 161.
4. M. MITOMO, F. IZUMI, Y. BONDO and Y. SEIKAWA, *Cer. Comp. Engng* (1983) 377.
5. J. WEISS and L. J. GAUCKLER, *J. Mater. Sci.* **10** (1981) 66.
6. G. Z. CAO, Z. K. HUANG, X. R. FU and D. S. YAN T. S. YEN, *Int. J. High Tech. Ceram.* **2** (1986) 115.
7. M. MITOMO, F. IZUMI, S. HORIUCHI and Y. MATSUI, *J. Mater. Sci.* **17** (1982) 2359.
8. E. M. LEVIN, C. R. ROBBINS and H. F. McMURDIE, in "Phase Diagrams for Ceramists 1969 Supplement" (National Bureau of Standards, American Ceramic Society, 1969) Figs 2340, 2341, 2372.
9. D. P. THOMPSON, in "Tailoring Multiphase and Composite Ceramics", edited by R. E. Tressler, G. L. Messing, C. G. Pantano and R. E. Newham (Plenum, New York, 1986) p. 79.
10. R. MARCHAND, A. JAYAWEERA and P. VERDIER, *J. Compt. Rend. Acad. Sci. Paris* **243** (1976) 675.
11. F. IZUMI, M. MITOMO and Y. BANDO, *J. Mater. Sci.* **19** (1984) 3115.
12. F. K. VAN DIJE, R. METSELLAAR and R. B. HELMHOLDT, *J. Mater. Sci. Lett.* **6** (1987) 1101.
13. R. D. SHANNON and C. T. PREWITT, *Acta Crystallogr.* **B25** (1969) 925.
14. T. EKSTRÖM, P.-O. KÄLL, M. NYGREN and P.-O. OLSSON, *J. Mater. Sci.* **24** (1989) 1853.
15. W. A. SANDERS and D. M. MIESKOWSKI, *Amer. Ceram. Soc. Bull.* **64** (1985) 304.
16. N. HIROSAKI, A. OKADA and K. MATOBA, *J. Amer. Ceram. Soc.* **71** (1988) c-144.
17. E. TANI, S. UMEBYASHI, K. KISHI, K. KOBAYASHI and M. NISHIJIMA, *Amer. Ceram. Soc. Bull.* **65** (1986) 1311.
18. I. C. HUSEBY and G. PETZOW, *ibid.* **59** (1980) 239.
19. P.-O. OLSSON, *J. Mater. Sci.* **24** (1989) 3878.
20. H. LARKER, in "Progress of Nitrogen Ceramics", edited by F. L. Riley (Martinus Nijhoff, The Hague, 1983) p. 717.
21. G. R. ANSTIS, P. CHANTIKUL, B. R. LAWN and D. P. MARSHALL, *J. Amer. Ceram. Soc.* **64** (1981) 533.
22. C. R. HUBBARD, H. E. SWANSON and F. A. MAUER, *J. Appl. Crystallogr.* **8** (1975) 45.
23. P.-O. KÄLL, *Chemica Scripta* **28** (1988) 439.
24. D. R. MESSIER, *Int. J. High Tech. Ceram.* **3** (1987) 33.
25. K. H. JACK, in "International Symposium on Non-Oxide and Technical and Engineering Ceramics", Limerick, edited by S. Hampshire (Elsevier Applied Science, 1986) p. 1.
26. A. MAKASHIMA, M. MITOMO, H. TANAKA, N. IL and M. TSUTSUMI, *Yogyo Kyokai Shi* **88** (1980) 701.
27. P. KORGUL and D. P. THOMPSON, personal communication, November, 1988.
28. S. HAMPSHIRE and M. POMEROY, personal communition, August, 1988.
29. C. GRESKOVICH and G. E. GAZZA, *J. Mater. Sci. Lett.* **4** (1985) 195.

Received 4 January
and accepted 7 June 1989